

ORIGINAL ARTICLE

Live imaging of induced and controlled DNA double-strand break formation reveals extremely low repair by homologous recombination in human cells

OD Shahar, EVS Raghu Ram, E Shimshoni, S Hareli, E Meshorer and M Goldberg

The Department of Genetics, The Institute of Life Sciences, The Hebrew University, Jerusalem, Israel

DNA double-strand breaks (DSBs), the most hazardous DNA lesions, may result in genomic instability, a hallmark of cancer cells. The main DSB repair pathways are non-homologous end joining (NHEJ) and homologous recombination (HR). In mammalian cells, NHEJ, which can lead to inaccurate repair, predominates. HR repair (HRR) is considered accurate and is restricted to S, G2 and M phases of the cell cycle. Despite its importance, many aspects regarding HRR remain unknown. Here, we developed a novel inducible on/off switch cell system that enables, for the first time, to induce a DSB in a rapid and reversible manner in human cells. By limiting the duration of DSB induction, we found that non-persistent endonuclease-induced DSBs are rarely repaired by HR, whereas persistent DSBs result in the published HRR frequencies (non-significant HR frequency versus frequency of ~10%, respectively). We demonstrate that these DSBs are repaired by an accurate repair mechanism, which is distinguished from HRR (most likely, error-free NHEJ). Notably, our data reveal that HRR frequencies of endonuclease-induced DSBs in human cells are >10-fold lower than what was previously estimated by prevailing methods, which resulted in recurrent DSB formation. Our findings suggest a role for HRR mainly in repairing challenging DSBs, in contrast to uncomplicated lesions that are frequently repaired by NHEJ. Preventing HR from repairing DSBs in the complex and repetitive human genome probably has an essential role in maintaining genomic stability.

Oncogene advance online publication, 21 November 2011; doi:10.1038/onc.2011.516

Keywords: DNA double-strand breaks; DNA repair; homologous recombination; genomic stability; *ISceI*

Introduction

DNA double-strand breaks (DSBs) are the most severe form of DNA damage since they may result in genomic instability, which is a hallmark of cancer cells. The two

major pathways that repair DSBs are non-homologous end joining (NHEJ) and homologous recombination (HR). In mammalian cells, NHEJ, which is based on rejoining of juxtaposed ends, predominates throughout the cell cycle and can lead to inaccurate repair. HR repair (HRR), which relies on a homologous DNA molecule, usually the sister chromatid, as a template, is considered accurate and is restricted to S, G2 and M phases of the cell cycle (Takata *et al.*, 1998; Rothkamm *et al.*, 2003; Saleh-Gohari and Helleday, 2004; Mao *et al.*, 2008; Shrivastav *et al.*, 2008; Hartlerode and Scully, 2009). In addition to being essential for DSB repair and for the maintenance of genomic stability, HR is important for directed gene targeting in gene therapy (Yanez and Porter, 1998).

HRR in human cells is widely studied using systems that are based on the combination of the overexpression of *ISceI* endonuclease and a reporter cassette. The commonly used DR-GFP reporter cassette contains the *ISceI* recognition sequence, which is absent in the human genome. A functional GFP is gained only if the *ISceI*-induced DSB is repaired by HR. Many discoveries were revealed using such systems, including finding HRR genes, the importance of the cell-cycle phase on the balance between HRR and NHEJ and the estimation that HRR frequency is 2–15% (Takata *et al.*, 1998; Pierce *et al.*, 1999; Rothkamm *et al.*, 2003; Saleh-Gohari and Helleday, 2004; Sartori *et al.*, 2007; Mao *et al.*, 2008; Shrivastav *et al.*, 2008; Hartlerode and Scully, 2009). It was suggested that repair of the *ISceI*-induced DSB in the DR-GFP cassette by NHEJ can destroy the *ISceI* site (Nakanishi *et al.*, 2005). However, the *ISceI*-induced DSB can also be repaired by error-free NHEJ, which restores the *ISceI* site. Thus, the DSB may repeatedly occur and be repaired as long as the endonuclease remains in the nucleus (Honma *et al.*, 2007; Mao *et al.*, 2008; Bennardo *et al.*, 2009). Such persistent DSBs may present a bias for data obtained using this system, which potentially allows an accurate repair of the initial DSB by NHEJ and repeated cycles of cleavage and repair. Hence, an HRR product may represent the repair of a DSB formed at later time points rather than the repair of the initial break. In addition, the described systems rely on the transfection efficiencies of an *ISceI*-expressing plasmid, resulting in a delay between the time of the transfection and the expression of an

Correspondence: Dr E Meshorer or Dr M Goldberg, The Department of Genetics, The Institute of Life Sciences, The Hebrew University, Givat Ram, Jerusalem 91904, Israel.

E-mail: meshorer@cc.huji.ac.il or goldbergm@vms.huji.ac.il

Received 17 May 2011; revised and accepted 11 October 2011

active enzyme. This time gap varies between cells in a given population and is difficult to monitor or quantify.

Here, we directly examined recurrence of DSB formation, and compared HRR following short-term versus persistent induction of DSBs, as well as the effect of the cell-cycle phase at the time of DSB formation on HRR. For these purposes, we developed an inducible and reversible live imaging-based cell system. By limiting the duration of DSB induction, we found that non-persistent *ISceI*-induced DSBs in human cells are rarely repaired by HR. We also found that these DSBs are mostly repaired by a different, error-free mechanism (most likely, NHEJ).

Results

Inducible and rapid generation of DSBs in human cells

In order to control the generation of an *ISceI*-induced DSB, we took advantage of the glucocorticoid receptor ligand binding domain (GRLBD) that rapidly translocates from the cytoplasm into the nucleus upon binding to ligands, such as Dexamethasone (Dex) or cortisol. A chimera between the *ISceI* endonuclease, the GRLBD and RFP was shown to induce an intact DNA damage response (Soutoglou *et al.*, 2007). For enhanced detection of the chimera under the microscope, we replaced the RFP with mCherry, generating a plasmid for the expression of mCherry fused to *ISceI* and GRLBD (Cherry-*ISceI*-GR). This plasmid was stably inserted into a U2OS cell line that stably carries the DR-GFP cassette (Sartori *et al.*, 2007), to create an inducible cell line for DSB generation in the DR-GFP cassette (HR-ind cells; Figure 1a).

Using time-lapse microscopy, we tracked the HR-ind cells for the mCherry signal. As expected, Cherry-*ISceI*-GR appeared solely in the cytoplasm in the absence of ligand (Figure 1b, upper left). As soon as 5 min after Dex addition, Cherry-*ISceI*-GR translocated to the nucleus and gradually accumulated therein (Figures 1b and c; Supplementary Movie 1). Due to the high affinity of Dex to the GRLBD, the Cherry-*ISceI*-GR was retained in the nucleus for a prolonged time (Figures 1b and c; Supplementary Figure 1), mimicking the fundamental features of the currently prevailing systems, while overcoming the drawbacks of endonuclease transfection. Nuclear localization of Cherry-*ISceI*-GR upon Dex addition resulted in the generation of DSBs at the DR-GFP cassette as determined by Ligation Mediated PCR (LM-PCR; Figure 1d; Supplementary Figure 2a).

DSB induction in HR-ind cells results in HRR

To directly analyze HRR of the *ISceI*-induced DSBs, we visualized the HR-ind cells using multicolor time-lapse microscopy for mCherry (Cherry-*ISceI*-GR) and GFP (indicating an HRR event in the DR-GFP cassette). We used polyclonal HR-ind cells to avoid clonal effects and to include cells lacking Cherry-*ISceI*-GR as an internal negative control under identical conditions within the same experiments. As expected, none of the Cherry-*ISceI*-GR-negative cells induced GFP expression upon

ligand addition (Figure 2a; Supplementary Movie 2). Nor was GFP expression detected when Cherry-*ISceI*-GR was restricted to the cytoplasm (Figure 2a). Upon activation of the HR-ind system by Dex, we detected the accumulation of GFP in a subset of Cherry-*ISceI*-GR-positive cells (Figure 2a; Supplementary Movie 2). Two days post Dex addition, ~7.5% of the HR-ind cells viewed under the microscope expressed GFP (Supplementary Table 1). A limiting factor of single cell analysis of a relatively rare process is the small amount of cells that can be examined. Therefore, we performed flow cytometry analysis to obtain HRR frequencies, 2 days post Dex addition to the HR-ind cells. Flow cytometry analysis showed an increase of 4.2% in GFP-positive cells upon Dex addition (Supplementary Figure 3; Figure 5a (right, no wash lane)). This HRR frequency is in agreement with previous reports based on cells transfected with an *ISceI* plasmid (Pierce *et al.*, 1999; Sartori *et al.*, 2007). Taken together, the HR-ind cells we generated combine a rapid induction of DSBs with an assay for HRR.

The GFP signal, resulting from HRR, can appear several cell divisions after Dex addition

GFP is observed as soon as 18 h after Dex addition with a variation on this time period between cells (Figure 2; Supplementary Movie 2). We occasionally detected cells that express GFP simultaneously (for example, Figures 2a and c; cells b or c2 and c3). Since HRR results in a genomic alteration, it is inherited by the daughter cells. Therefore, HRR before cell division can lead to GFP expression in the mother and daughter cells (Figure 2c; cell b). However, if HRR occurs shortly before division, not allowing sufficient time for GFP accumulation, only the daughter cells display GFP (referred to as pre-division repair; Figure 2c; cell c). HRR can also occur after division, resulting in one GFP-positive and one GFP-negative daughter cell (Figure 2c; cell a). Moreover, expression of GFP due to HRR does not necessarily appear in the same cell cycle in which Dex was added and it can appear after sequential cell-cycle divisions (Supplementary Table 2). Also, the proportion of cells, out of all cells expressing GFP, in which pre-division repair occurred, was measured (Supplementary Table 2). Hence, HRR can occur at different time points after Dex addition.

Since HRR is affected by the cell cycle (Takata *et al.*, 1998; Rothkamm *et al.*, 2003; Mao *et al.*, 2008; Takashima *et al.*, 2009), we examined the cell-cycle profile of the HR-ind cells by flow cytometry analysis of DNA content. An intact cell-cycle profile was observed and no significant difference between mCherry-negative and mCherry-positive cells was detected (Supplementary Figures 4a and b). Furthermore, we confirmed that *ISceI* induces similar levels of DSBs in different cell-cycle phases (Supplementary Figure 4c).

HRR is observed in HR-ind cells, in which the initial DSB was induced in different cell-cycle phases, including G1

Previous studies revealed that while DSB repair by NHEJ is predominant throughout the cell cycle, HRR is

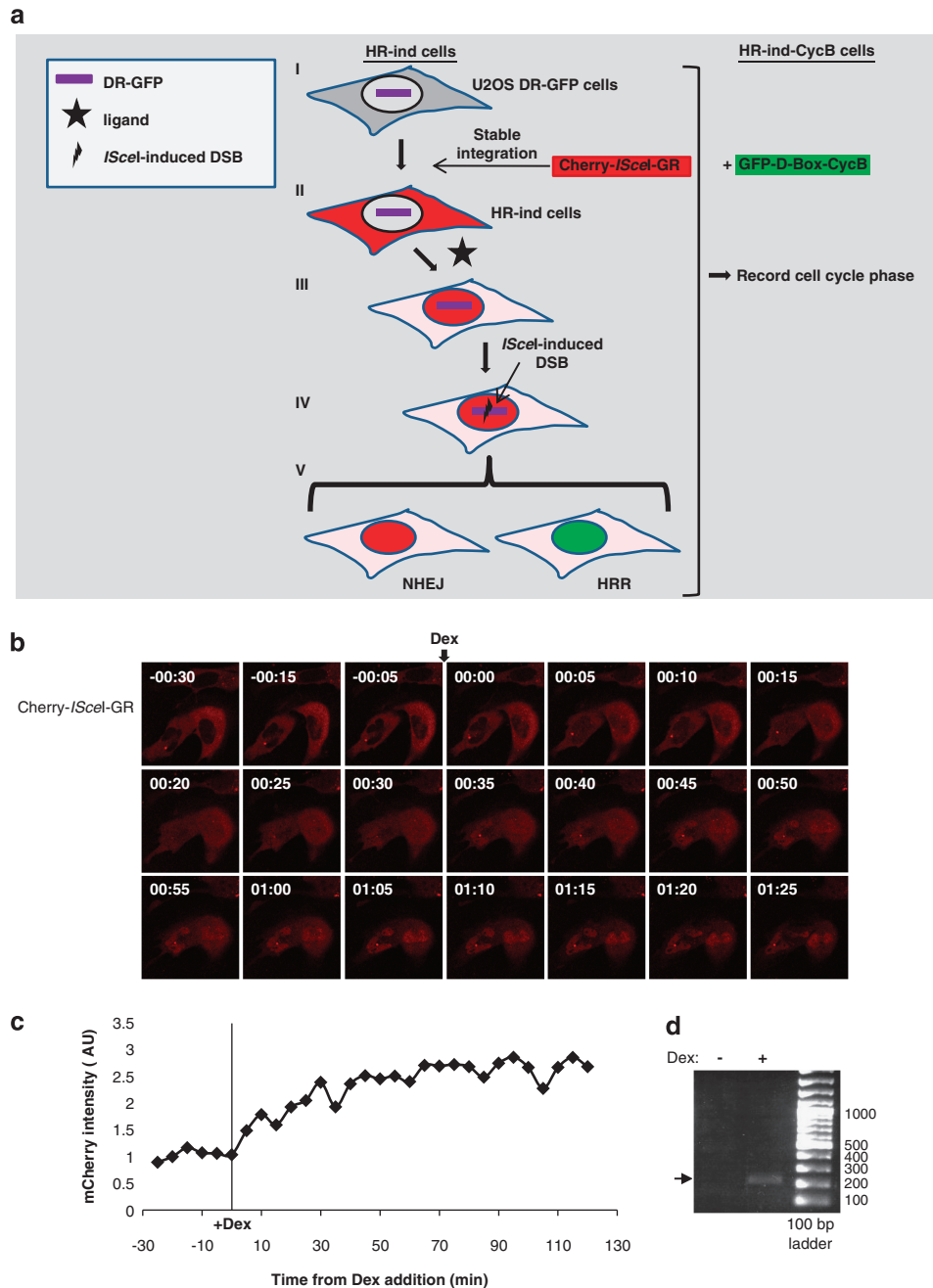


Figure 1 DSB induction and visualization in HR-ind cells. **(a)** Schematic representation of the HR-ind cell system. Left: HR-ind cells. (I) U2OS DR-GFP cells were stably transfected with Cherry-*I*SceI-GR to generate the HR-ind cells. (II) Cherry-*I*SceI-GR is cytoplasmic. (III) Upon ligand addition, it rapidly translocates into the nucleus. (IV) The endonuclease generates a DSB at the *I*SceI site in the DR-GFP cassette. (V) This DSB can be repaired by NHEJ (red nucleus) or by HRR (green nucleus, nuclear GFP is expressed due to an HRR event at the DR-GFP cassette). Right: HR-ind-CycB cells. HR-ind cells were infected with GFP-D-Box-CycB. The cell-cycle phase of the HR-ind-CycB cells can be recorded before, during and after ligand addition. **(b)** Visualization of Cherry-*I*SceI-GR in HR-ind cells before (–min) and after Dex addition. **(c)** A plot of mCherry fluorescence intensity (arbitrary units, AU) versus time (min) in the nucleus of the lower right cell is shown in **(b)**. **(d)** LM-PCR of HR-ind cells before (–) and 30 min after Dex addition (+). Arrow indicates the 207-bp product representing *I*SceI-induced DSBs.

restricted to S, G2 and M phases (Takata *et al.*, 1998; Rothkamm *et al.*, 2003; Mao *et al.*, 2008; Takashima *et al.*, 2009). The connection between DSB repair and cell-cycle phase was mainly studied with cells synchronized to a specific phase, using methods, which by themselves induce DNA damage (Takata *et al.*, 1998;

Rothkamm *et al.*, 2003; Mao *et al.*, 2008; Takashima *et al.*, 2009). In order to further study the effect of cell-cycle phase on HRR, in cells with an intact cell-cycle progression, we developed an *in-silico* synchronization system by introducing a reporter for S, G2 and M phases to mark cells that can potentially repair DSBs by

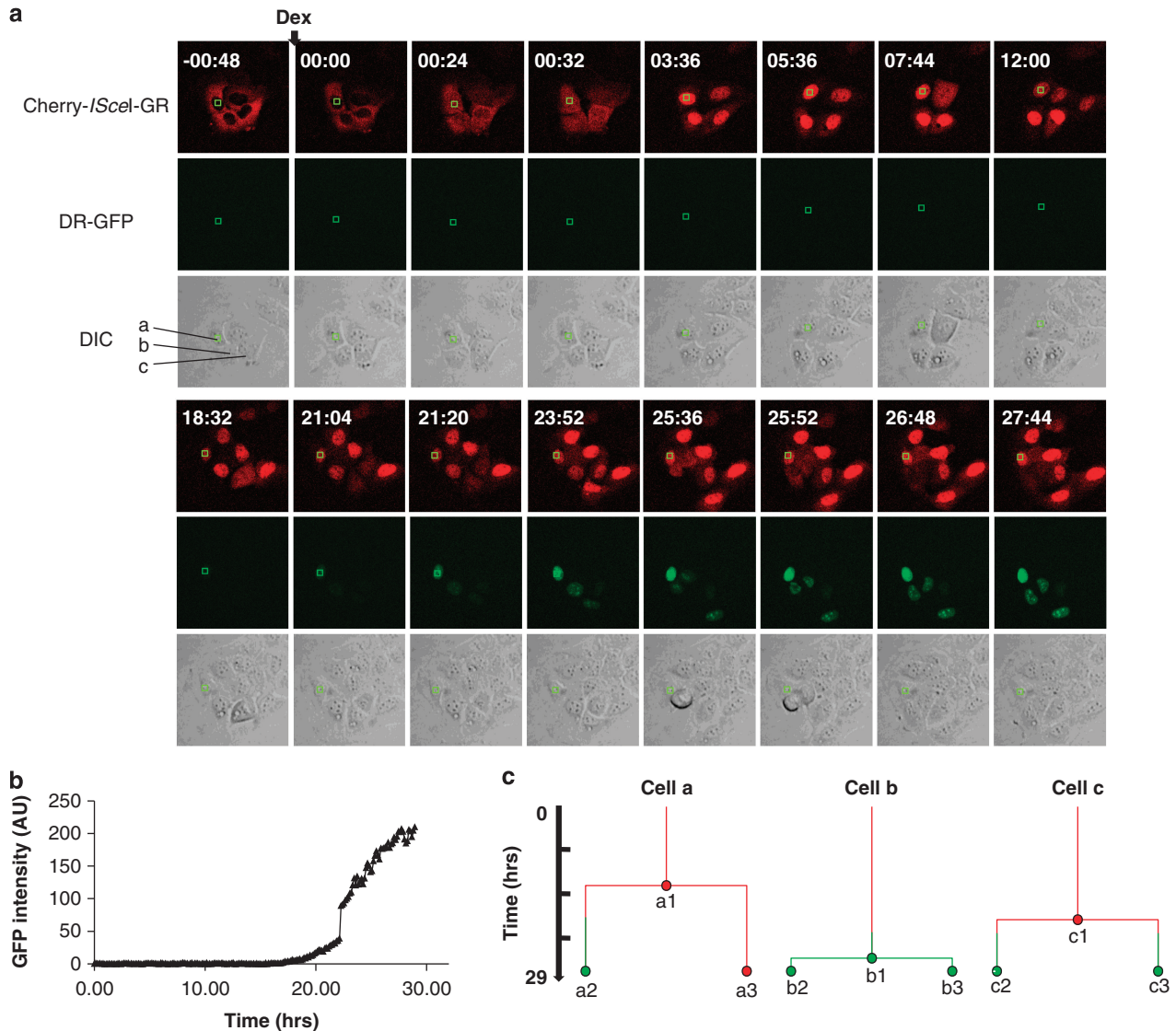


Figure 2 Visualization of HRR by *ISceI*-induced DSBs in HR-ind cells. **(a)** Time-lapse microscopy images of HR-ind cells. Cherry-*ISceI*-GR: In the absence of Dex, Cherry-*ISceI*-GR is cytoplasmic (–00:48, 00:00), it translocates into the nucleus within minutes after Dex addition (00:24, 00:32), and accumulates therein (03:20–27:44). DR-GFP: Repair of the *ISceI*-induced DSB at the DR-GFP cassette results in the expression of nuclear GFP. No GFP is detected before Dex addition or in the hours to follow (–00:48–18:32). GFP expression in some cells is detected (21:04–27:44). Green square indicates the nuclear ROI in which GFP fluorescence intensity was measured. **(b)** A plot of GFP median intensity (AU) in the indicated ROI of cell ‘a’ (a) versus time (hours). **(c)** A tree diagram of three representative cells (cells a, b and c (a)), describing the cells’ lineage as detected by time-lapse microscopy. Nodes represent cell divisions, and the line color represents cells expressing (green) or not expressing (red) GFP.

HR. The reporter includes the destruction box of Cyclin B fused to GFP (GFP-D-Box-CycB) that is constitutively transcribed and is regulated by degradation (Chang *et al.*, 2003; Fung and Poon, 2005). GFP-D-Box-CycB is absent in G1, begins to accumulate during S phase, accumulates further during G2/M and disappears at the end of mitosis (Brandeis and Hunt, 1996; Zur and Brandeis, 2001). Introducing GFP-D-Box-CycB into the HR-ind cells yielded a cell line that combines the ability to track in real time the cell cycle, induce DSBs and analyze HRR (referred as HR-ind-CycB; Figure 1a). We could easily distinguish between the signals of DR-GFP and GFP-D-Box-CycB. The

DR-GFP signal is strong, constant, restricted to the nucleus and present in both daughter cells after division (Figure 3a; Supplementary Movie 2), in contrast to the oscillatory signal of GFP-D-Box-CycB that completely disappears following division (Figure 3a; Supplementary Movie 3).

We added Dex to the HR-ind-CycB cells and tracked the GFP signal. The GFP signal at the time of Dex addition reflects the cell-cycle phase, since there is no GFP due to HR (DR-GFP) at this time point. DR-GFP expression was observed in cells in which the initial DSB was induced in different phases of the cell cycle, including G1 (Figures 3b–d; Supplementary Movies 4

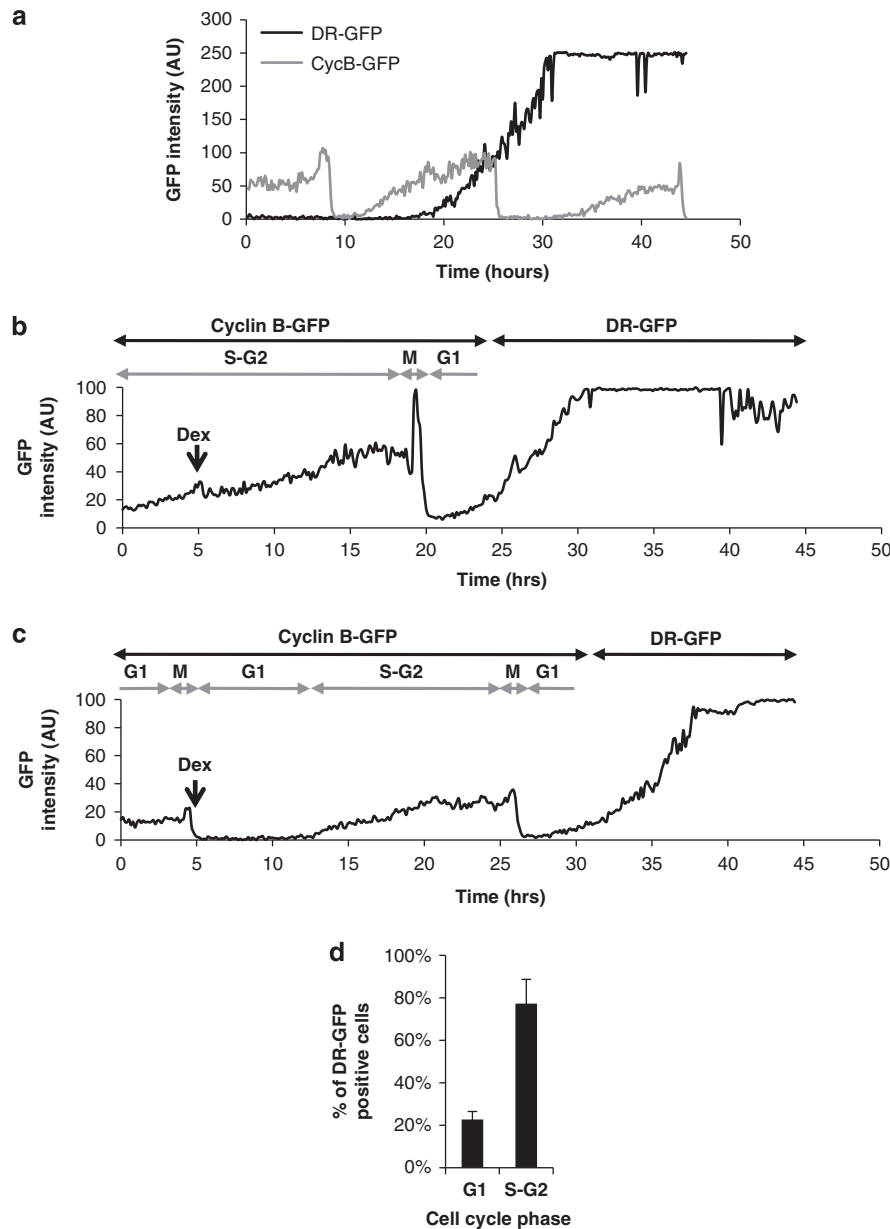


Figure 3 HRR is observed in HR-ind cells in which the initial DSB was induced in different phases of the cell cycle. **(a)** GFP signal of GFP-D-Box-CycB is distinguished from DR-GFP. Plots of intensities in nuclear ROI versus time are shown. Black denotes GFP signal obtained due to HRR event in an HR-ind cell treated with Dex (DR-GFP). Note that the expression is steady. Gray indicates GFP signal of GFP-D-Box-CycB in a nuclear ROI in an HR-ind-CycB cell (no treatment with Dex). Note that the signal is oscillatory and drops at the end of mitosis. **(b, c)** HRR events upon Dex addition at different phases of the cell cycle. Plots of GFP intensity (AU) versus time (hours) in two HR-ind-CycB cells that resulted in HRR: a cell that was at S/G2 **(b)** and a cell that was at the beginning of G1 **(c)** at the time of Dex addition: (0504 h). **(d)** Quantification of cells according to their cell-cycle phase at the time of initial DSB formation. Percent out of the DR-GFP-positive cells (repaired by HR) in each cell-cycle phase as recorded by multi-color time-lapse microscopy. An average of at least three independent experiments is shown. $N > 30$.

and 5). Thus, activation of the HR-ind-CycB cells by Dex in G1 can result in an HR event, which probably occurs during S, G2 or M. This implies that the initial DSB was repaired during G1 by an accurate repair mechanism that restored the *ISceI* site, which then was subjected to recurrent DSB formation. This may suggest that a prolonged retention of the endonuclease in the nucleus (due to transfection of an *ISceI*-expression plasmid or the activation of HR-ind cells by Dex) allows

recurrent DSB induction. The accurate repair mechanism is not HR as HRR of an *ISceI*-induced DSB at the DR-GFP cassette abolishes the *ISceI* site (Pierce *et al.*, 1999). Since NHEJ in human cells is the predominant repair pathway (Hartlerode and Scully, 2009), it is most likely that these DSBs are repaired by error-free NHEJ. Hence, HRR of a DSB induced in G1 is probably a result of recurrence of the DSB at the *ISceI* site at later time points (during S, G2 or M).

Retention of ISceI in the nucleus results in persistent DSB formation

To achieve a temporary, short-term cleavage of the *ISceI* site by Cherry-*ISceI*-GR, we took advantage of the natural ligand cortisol, which is less stable and has a lower affinity to the GRLBD, compared with Dex

(Schaaf and Cidlowski, 2003). Therefore, removal of cortisol from the media should result in clearance of Cherry-*ISceI*-GR from the nucleus. Addition of cortisol resulted in a rapid translocation of Cherry-*ISceI*-GR from the cytoplasm into the nucleus (Figures 4a and b; Supplementary Movie 6), similarly to Dex addition.

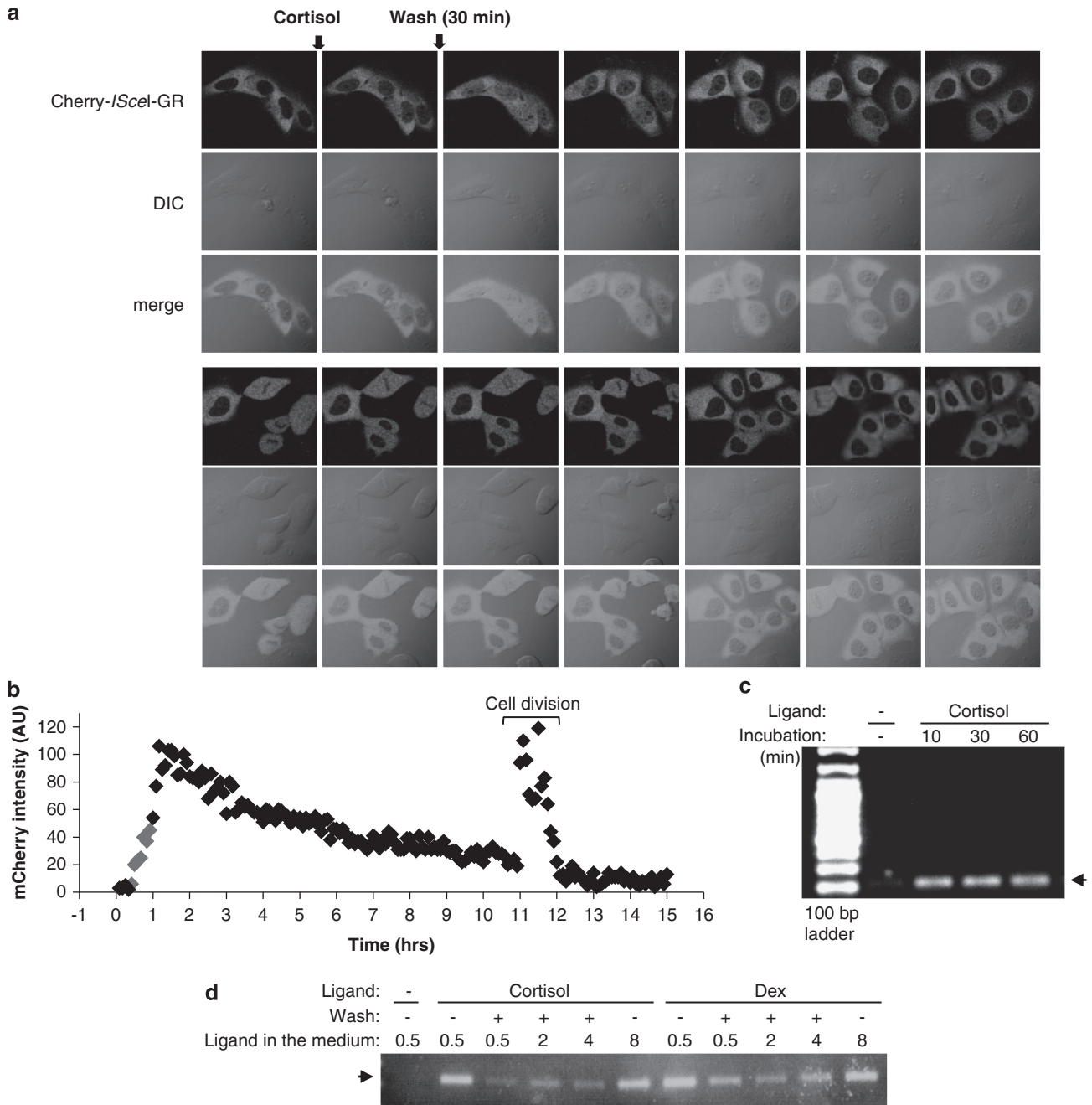


Figure 4 Recurrence of DSBs upon prolonged nuclear retention of *ISceI*. **(a)** Time-lapse images showing translocation of Cherry-*ISceI*-GR into the nucleus upon cortisol addition (00:20–01:05), and its clearance from the nucleus several hours after cortisol removal (03:00–10:55). **(b)** Quantification of mCherry intensity (AU) in the nucleus of a representative cell over time (hours). Gray dots indicate time points in which the cells were incubated with cortisol. **(c)** DSBs formation upon addition of cortisol. Cells were incubated with cortisol 10, 30 or 60 min and DNA was extracted after ligand addition followed by LM-PCR. **(d)** Repeated cycles of DSB formation and repair, and abolishment of DSBs formation upon cortisol removal. Semiquantitative LM-PCR is shown. HR-ind cells were incubated with ligands (Cortisol or Dex). Cells were either left with the ligand (Wash: –) for 0.5 or 8 h or washed (+) after 0.5, 2 or 4 h and incubated in ligand-free media for 7.5, 6 or 4 h, respectively. This allows different durations for Cherry-*ISceI*-GR clearance from the nucleus and for DSB repair. DNA was extracted 0.5 h after ligand addition (no wash, 0.5 h) or 8 h after ligand addition (all the rest). Arrow indicates the 207-bp product representing *ISceI*-induced DSBs (c, d).

Semiquantitative LM-PCR confirmed induction of DSBs in the *ISceI* site as early as 10 min after cortisol addition (Figure 4c; Supplementary Figure 2). These cortisol-induced DSBs were repaired by HR in similar frequencies to DSBs induced by Dex (Supplementary Table 2). To remove cortisol, we washed the cells 30 min after its addition and added cortisol-free media. This blocked the entrance of Cherry-*ISceI*-GR into the nucleus and the enzyme was retained in the cytoplasm. A decrease in the Cherry-*ISceI*-GR levels in the nucleus was visible from ~2 h after cortisol removal (Figures 4a and b; Supplementary Figure 5; Supplementary Movie 6). Subsequent to cell division, even if it occurs shortly after the removal of cortisol from the media, no Cherry-*ISceI*-GR appears in the nuclei of the daughter cells (Supplementary Movie 6). Therefore, we developed a cell system that enables for the first time to induce a DSB in a reversible and controlled manner.

If removing the cortisol stops recurrence of DSBs, we expect to observe less DSBs after the initial cleavage is repaired in comparison with cells, in which Cherry-*ISceI*-GR remains in the nucleus and continuously generates DSBs. To test this, we analyzed the levels of *ISceI*-generated DSBs. Washing the cortisol 30 min after its addition and allowing the cells 7.5 h to repair the cleavage resulted in a significant reduction of DSBs at the DR-GFP cassette, in contrast to a similar treatment with the stable ligand Dex, which resulted only in a slight decrease in DSBs (Figure 4d). This observation, together with the finding that HRR can occur in cells in which the initial DSB was induced in G1 (Figures 3c and d), suggests a robust role for an accurate repair mechanism in human cells, which is distinct from HR.

Prolonged nuclear retention of *ISceI* results in HRR

We further examined HRR during different durations of DSBs induction (Supplementary Figure 6). Analysis of HRR events 2 days following Dex or cortisol addition, using flow cytometry, revealed frequencies of 4.2 or 3.1%, respectively (Figure 5a; no wash). We hypothesized that the higher frequency of HRR events obtained upon Dex addition, is an outcome of Dex being more stable than cortisol (Schaaf and Cidlowski, 2003), resulting in more DSBs that reoccurred at later time points. If ligand stability is a limiting factor, then adding fresh ligand at later time points should increase HRR events. Indeed, replenishing cells with fresh media containing Dex or cortisol at the initial concentrations increased HR efficiencies to 5.5 or 4.1%, respectively (Figure 5a; freshly added). This implies that the prolonged presence of *ISceI* in the nucleus is important for HRR events rather than its initial concentration.

Short-term generation of *ISceI*-induced DSBs rarely results in HRR

Next, we analyzed HRR events following short-term induction of DSBs. Surprisingly, when using cortisol and washing it after 10 or 30 min, we did not detect cells expressing DR-GFP by live imaging (Supplementary Movie 7), despite the production of DSBs at the

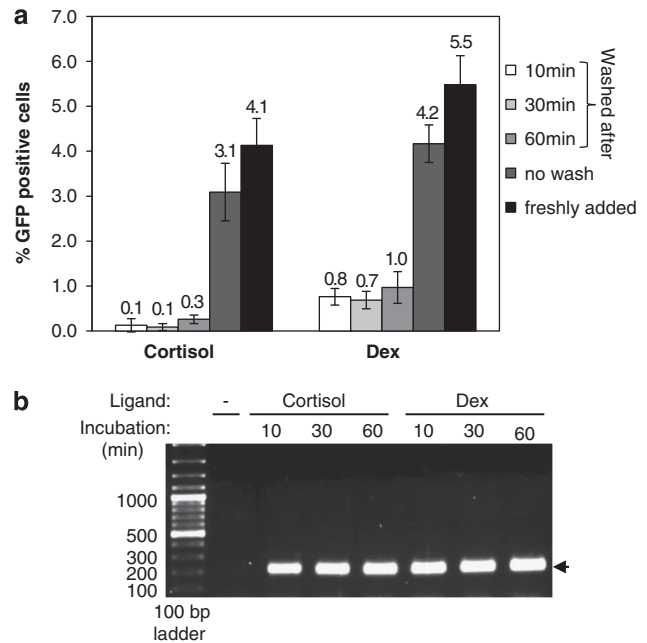


Figure 5 Induction of DSBs for short duration at the DR-GFP cassette results in extremely low frequencies of HRR. (a) Quantification of flow cytometry analysis for HR product (GFP). HR-ind cells were incubated with cortisol or Dex and washed after the indicated times, or not washed at all (no wash), and subjected to flow cytometry analysis after 2 days (at least three independent experiments were done). Media was replaced with fresh media containing the initial concentration of cortisol or Dex after 5, 10 and 24 h (freshly added). Bars indicate s.e.m. (b) DSBs formation upon ligand addition for the indicated periods. Cells were incubated with cortisol or Dex for 10, 30 or 60 min and DNA was extracted 60 min after ligand addition followed by LM-PCR. Arrow indicates the 207-bp product representing *ISceI*-induced DSBs.

DR-GFP cassette (Figure 4c). This suggests that no HRR events occurred in the *ISceI* site following this short-term cleavage. The effect of short-term cleavage on HRR was so strong that it ruled out the possibility to analyze the influence of short-term DSB induction in different phases of the cell cycle on HRR.

To confirm that the lack of HRR is not due to the relatively small amount of cells sampled by live imaging, we performed flow cytometry analysis to determine HRR frequencies upon short-term DSB formation in HR-ind cells. In agreement with the results obtained by live imaging, no significant increase in GFP-positive cells (HRR) was detected upon cortisol addition for 10, 30 or 60 min using flow cytometry analysis (Figure 5a). Notably, similar treatments with the non-washable ligand Dex resulted in HRR (Figure 5a). This difference was obtained despite similar DSBs formation upon short induction by cortisol or Dex (Figure 5b). Still, HRR frequencies in cells incubated with Dex for 10, 30 or 60 min followed by removal of the ligand from the media were lower compared with cells in which the ligand was retained in the media (Figure 5a). Hence, our results demonstrate that HRR frequencies of *ISceI*-generated DSBs are much lower than previously reported. The bias for higher HRR probably arises from persistent DSBs obtained by previous methods.

To examine the biological relevance of the HR-ind system, we analyzed the effect of silencing NHEJ or HR genes on HRR frequencies in the system. As expected, downregulation of Ku80, which is a key member of NHEJ, increased HRR frequency. In contrast, downregulation of Rad51, which is essential for HRR, reduced HRR of DSBs formed by cortisol addition (Supplementary Figure 7; cortisol). Remarkably, downregulation of either Ku80 or Rad51 had no effect on HRR efficiencies following short-term induced DSBs (Supplementary Figure 7; cortisol wash). Taken together, our results reveal that HRR frequency of *ISceI*-generated DSBs is very low and suggest that persistent DSB formation is required for HRR.

Discussion

In this study, we demonstrate that non-persistent *ISceI*-induced DSBs are rarely repaired by HR, whereas the repair of persistent DSBs results in the published HRR frequencies. We also show that *ISceI*-induced DSBs are repaired by an error-free mechanism, which is distinguished from HRR.

The inducible cell system we developed allows studying HRR of a rapid and temporal *ISceI*-generated DSB in living human cells in real time. The system overrides many drawbacks of previously reported methodologies, which rely on transfection of the *ISceI*-expressing plasmid and in which the *ISceI* is retained for prolonged time in the nucleus. It allows, for the first time, to monitor living cells before a DSB is formed, during DSBs formation, and to track cells that accumulate GFP as a result of HRR. Combining these advantages with *in-silico* cell-cycle synchronization (Figure 1a) provides novel tools for confronting long sought-after questions regarding HRR of DSBs in human cells. The described cell system will facilitate screens for HRR genes, by overriding the faults of transfections. Furthermore, it will enable analyzing HRR kinetics and discovering novel genes involved in it. Notably, our study provides a proof of concept for the ability to activate steroid hormone receptors, widely used as vehicles to transfer proteins from the cytoplasm into the nucleus, in a reversible manner.

The juxtaposed DNA ends, formed by the endonuclease, are in the context of chromatin and the cellular environment, which include enzymes and free radicals. Therefore, they are constantly exposed to chemical alterations and may obtain chemical modifications of the base, sugar or phosphate components near the break, resulting in the loss of the original sequence. Such alterations may preclude ligation, which is essential for NHEJ (Covo *et al.*, 2009). The effect of NHEJ impairment on HRR may provide a hint regarding the biological relevance of such DSBs in our cells. The fact that downregulation of Ku80 impairs the balance between NHEJ and HRR (Supplementary Figure 7; cortisol), suggests that the 'clean' nature of the DSB does not last forever. Otherwise, it could have been easily ligated again requiring only a ligase activity, and not utilize the complex cellular repair machinery.

Here, we demonstrate that prolonged retention of *ISceI* in the nucleus results in recurrence of DSBs formation at the *ISceI* site. This indicates restoration of the *ISceI* site by an accurate repair, via a pathway which is distinct from HR, and which most probably involves an error-free NHEJ repair mechanism (Supplementary Figure 8). Previous studies, in which the *ISceI* site was found to be destroyed upon NHEJ repair, likely involved persistency of DSB induction due to *ISceI* transfection. We suggest that the *ISceI*-induced DSBs are often repaired accurately. Since events that result in non-accurate repair destroy the *ISceI* site, they prevent any potential DSB formation and become end products. This is likely to be the case, since the detection of non-accurate repair products in previous studies was subsequent to PCR amplification, thereby even if few such non-accurate molecules are generated they will be detected (Nakanishi *et al.*, 2005). If the *ISceI* is retained for a prolonged time in the nucleus, as in previous systems, such non-accurate events are likely to occur. This probably affects some of the studies that relied on overexpressing endonucleases (such as, *ISceI*) for DSB induction, since they do not allow determining if the HRR product results from the initial DSB or breaks that occurred at later time points (Supplementary Figure 8). In fact, we found that the repair frequency of *ISceI*-generated DSBs by HR is considerably lower than previously reported (Figure 5a). Our results propose that DSBs are rarely repaired by HR in human cells and may explain the low efficiency of directed gene targeting, which is based on HR (Yanez and Porter, 1998). We suggest that the *ISceI*-induced DSBs that are eventually repaired via HRR are DSBs that went through repeated cycles of DSB formation and repair.

According to our proposed model (Supplementary Figure 8), most DSBs are repaired by NHEJ. A DSB that is hard to repair, modeled here by the recurrence of the DSB, is occasionally repaired by HR. It was suggested in yeast that the type of DSB, rather than the cell-cycle phase at the time of induction, determines the repair pathway. 'Clean' DSBs (induced by an endonuclease) are repaired by NHEJ while 'ragged' DSBs (induced by ionizing radiation) are marked for subsequent repair by HR during S-G2 (Barlow *et al.*, 2008). It is possible that persistent DSBs mimic 'hard-to-repair DSBs', thereby triggering HRR. Persistent DNA damage may increase the probability to obtain chemical modifications. Alternatively, a mechanism that is sensitive to DSB duration at specific loci might exist, but is yet to be found. This may explain the HRR frequencies observed in systems in which *ISceI* is active for prolonged durations. The results may strongly affect the dogma regarding DSB repair in human cells, as it seems that HR is only used to repair DSBs which could not be repaired by NHEJ. Therefore, HRR is not a mechanism that works side by side with NHEJ, rather it serves to repair complicated lesions modeled here by persistent DSBs. Our model is strengthened by a recent study in which DSB formation was induced in cells by different DNA damage agents (high linear energy transfer carbon ions, X-rays and etoposide) and the

sequential recruitment of HR or NHEJ proteins to DSBs was analyzed (Shibata *et al.*, 2011). The authors concluded that NHEJ makes the first attempt to repair DSBs. If the subsequent steps of NHEJ can progress, then the DSB will be repaired by NHEJ. However, if rapid rejoining cannot ensue either due to DNA lesion or chromatin complexity, then the DSB will be repaired by HR during the G2 phase (Shibata *et al.*, 2011).

The human genome contains a high fraction of repetitive sequences. Hence, HRR may lead to genomic instability if a wrong homologous sequence is chosen for repair (Jeggo, 1998), and result in cancer or other genomic instability-related diseases. Indeed, NHEJ is the prominent DSB repair machinery in human cells. We suggest that DSBs repaired via HR are mainly those which could not be repaired by NHEJ. Such DSBs may be lesions that are hard to repair, or recurring DSBs that are formed at specific loci, modeled by the HR-ind system. It can be speculated that persistent DSBs may occur, for example, at fragile sites. These loci challenge the replication machinery, occasionally resulting in replication fork collapses that can generate DSBs (Lukusa and Frys, 2008). Accordingly, under conditions that slow DNA replication, both HRR and NHEJ pathways are activated to maintain fragile site stability (Schwartz *et al.*, 2005).

In conclusion, we used a novel on/off switch inducible cell system for studying HRR of a rapid and temporal generated DSB. Single cell analysis allowed us to monitor living cells before a DSB is formed, during DSBs formation, and to track cells that accumulate GFP as a result of HRR. Using this cell system, we demonstrated that non-persistent endonuclease-induced DSBs are rarely repaired via HR.

Materials and methods

Plasmids and cell lines. Cherry-*I SceI*-GR was cloned by cutting *I SceI*-GR from RFP-*I SceI*-GR (obtained from T Misteli, National Cancer Institute; Soutoglou *et al.*, 2007) with *Bam*HI/*Sae*I and ligating it into pmCherry-C1. To generate the HR-ind cells, U2OS-DR-GFP cells (obtained from SP Jackson, University of Cambridge; Sartori *et al.*, 2007) were transfected with the Cherry-*I SceI*-GR plasmid. The cells were selected with 0.4 µg/ml G418 (BD Biosciences) for 2 weeks. Stable cells were retained in the 0.2-µg/ml G418 and 1-µg/ml puromycin. To obtain HR-ind-CycB cells, GFP-D-Box-CycB plasmid, which contains GFP fused to Cyclin B destruction box under the *pgk* promoter (obtained from A Klochendler-Yeivin and A Eden, The Hebrew University; Salpeter *et al.*, 2011), was infected to HR-ind cells by lentiviruses. Viral particles were produced as described (Moffat *et al.*, 2006) and target cells were exposed to two rounds of infection. mCherry-positive cells were sorted using FACSVantageSE cell sorter (Becton Dickinson, Franklin Lakes, NJ, USA). All cells were maintained in DMEM (without phenol red) containing 10% fetal calf serum (charcoal treated), L-glutamine 20 mM, penicillin 500 units/ml and streptomycin 0.5 mg/ml (Biological Industries, Beit Haemek, Israel), 37 °C and 5% CO₂. mCherry-positive cells were enriched by sorting with FACSVantageSE cell sorter (Becton Dickinson).

Ligation Mediated PCR. LM-PCR was done after Villalobos *et al.* (2006). HR-ind cells were harvested and genomic DNA was purified using the genomic DNA isolation kit (Sigma, Rehovot, Israel). In all, 1 µg of DNA was ligated with 100 pmol of an asymmetric adaptor (5'phosphate-CTAC AGATCAGGCGTCTGTCTGCTCATG) and (CATGA GCACGACAGACGCCTGATCTGTAGTTAT) at 18 °C for 22 h. PCR was carried out using 25 ng of ligated template per reaction and an adaptor primer CGACAGACGC CTGATCTGTA and a GFP primer ATCAGGCAGAGC AGGAACCTGAG. For semiquantitative PCR, the products were normalized to β-actin. β-actin PCR was carried out using primers B-ActF-TTCTACAATGAGCTGCGTGTGGCT and B-ActR-AACGGCAGAAGAGAGAACCAGTGA. The linear range of amplification was used to determine the number of cycles for the *I SceI*-induced DSBs positive product and β-actin. Samples were recovered during the linear phase of amplification and quantization of PCR bands from the 1.2% agarose gel was carried out using ImageJ (NIH, Bethesda, MD, USA).

Live imaging. Cells were placed on an 8 µ slide (ibidi, Applied BioPhysics, Inc., Troy, NY, USA). Imaging was performed using either a Revolution spinning disk (CSUX) imaging system (Andor, Belfast, UK) with solid state lasers 488 and 561 nm (50 mW each) or using an Olympus FV1000 confocal microscope (Olympus, Tokyo, Japan) with a 488-nm Argon ion laser and a 543-nm solid state laser, emissions filters were 505–525 or 560–620 nm, respectively. Both mounted on an Olympus IX81 fully automated microscope equipped with an automated stage, auto-focus device (Z-drift compensation, ZDC) and an environmental chamber (LIS, Switzerland) controlling oxygen, humidity, CO₂ and temperature. A ×60/1.4 oil immersion or ×20/0.75 air objectives were used. Differential interference contrast image were also taken. The images were taken every 5 or 8 min. Data analysis was performed using ImageJ (NIH). Manual tracking was used for tracking cells and a macro was written to allow median calculation in a region of interest (ROI) of 9 or 11 pixels square edges. A script was written in Matlab to draw tree plots according to GFP detection times and cells division time points.

HR assay. Activation of the HR-ind cells was done by addition of 10⁻⁷ M Dex or 10⁻⁶ M cortisol. Analyzing GFP-positive cells out of the mCherry-positive cells in flow cytometric analysis was done using SORP LSRII cell analyzer or FACScalibur (Franklin Lakes, NJ, USA), similarly to Sartori *et al.* (2007). Since the Cherry-*I SceI*-GR is stably expressed, no transfection or normalization was required.

Cell-cycle analysis. Cells were incubated with 5 µg/ml Hoechst-33342 (Molecular Probes, Eugene, OR, USA) for 20 min. Following extraction, cells were analyzed using flow cytometry (SORP LSRII) for DNA content (UV 355 nm, 60 mW laser), and mCherry (561 nm, 25 mW laser) using Cellquest or FlowJo programs. Doublets were discriminated as described (Wersto *et al.*, 2001). Watson model was used to fit cell-cycle profile.

Conflict of interest

The authors declare no conflict of interest.

Acknowledgements

We thank members of our laboratories, Sagiv Shifman and Liran Carmel for discussions, Naomi Melamed-Book for assistance in confocal analyses, Maya Schuldiner and Yifat Cohen for technical help. Stephan P Jackson, Tom Misteli, Amir Eden and Agnes Klochendler-Yeivin for reagents, Ilana Livyatan for critical reading of the manuscript, Evi Soutoglou for discussions and reagents, and the Edmond J Safra Foundation for financial support. MG is supported

by the AFHU, The United States Binational Science Foundation (2009286) and the Israel Cancer Association. EM is a Joseph H and Belle R Braun senior lecturer in life sciences and is supported by the Israel Science Foundation (943/09), the Israel Cancer Research Foundation, the Israel Ministry of Health (6007), the European Union (IRG-206872 and 238176), the Internal Applicable Medical Grants of the HU and the Israel Psychobiology Institute. EVSRR is supported by the Lady Davies Fellowship program.

References

- Barlow JH, Lisby M, Rothstein R. (2008). Differential regulation of the cellular response to DNA double-strand breaks in G1. *Mol Cell* **30**: 73–85.
- Bennardo N, Gunn A, Cheng A, Hasty P, Stark JM. (2009). Limiting the persistence of a chromosome break diminishes its mutagenic potential. *PLoS Genet* **5**: e1000683.
- Brandeis M, Hunt T. (1996). The proteolysis of mitotic cyclins in mammalian cells persists from the end of mitosis until the onset of S phase. *EMBO J* **15**: 5280–5289.
- Chang DC, Xu N, Luo KQ. (2003). Degradation of cyclin B is required for the onset of anaphase in Mammalian cells. *J Biol Chem* **278**: 37865–37873.
- Covo S, de Villartay JP, Jeggo PA, Livneh Z. (2009). Translesion DNA synthesis-assisted non-homologous end-joining of complex double-strand breaks prevents loss of DNA sequences in mammalian cells. *Nucleic Acids Res* **37**: 6737–6745.
- Fung TK, Poon RY. (2005). A roller coaster ride with the mitotic cyclins. *Semin Cell Dev Biol* **16**: 335–342.
- Hartlerode AJ, Scully R. (2009). Mechanisms of double-strand break repair in somatic mammalian cells. *Biochem J* **423**: 157–168.
- Honma M, Sakuraba M, Koizumi T, Takashima Y, Sakamoto H, Hayashi M. (2007). Non-homologous end-joining for repairing I-SceI-induced DNA double strand breaks in human cells. *DNA Repair (Amst)* **6**: 781–788.
- Jeggo PA. (1998). DNA breakage and repair. *Adv Genet* **38**: 185–218.
- Lukusa T, Fryns JP. (2008). Human chromosome fragility. *Biochim Biophys Acta* **1779**: 3–16.
- Mao Z, Bozzella M, Seluanov A, Gorbunova V. (2008). DNA repair by nonhomologous end joining and homologous recombination during cell cycle in human cells. *Cell Cycle* **7**: 2902–2906.
- Moffat J, Grueneberg DA, Yang X, Kim SY, Kloepfer AM, Hinkle G *et al.* (2006). A lentiviral RNAi library for human and mouse genes applied to an arrayed viral high-content screen. *Cell* **124**: 1283–1298.
- Nakanishi K, Yang YG, Pierce AJ, Taniguchi T, Digweed M, D'Andrea AD *et al.* (2005). Human Fanconi anemia monoubiquitination pathway promotes homologous DNA repair. *Proc Natl Acad Sci USA* **102**: 1110–1115.
- Pierce AJ, Johnson RD, Thompson LH, Jasin M. (1999). XRCC3 promotes homology-directed repair of DNA damage in mammalian cells. *Genes Dev* **13**: 2633–2638.
- Rothkamm K, Kruger I, Thompson LH, Lobrich M. (2003). Pathways of DNA double-strand break repair during the mammalian cell cycle. *Mol Cell Biol* **23**: 5706–5715.
- Saleh-Gohari N, Helleday T. (2004). Conservative homologous recombination preferentially repairs DNA double-strand breaks in the S phase of the cell cycle in human cells. *Nucleic Acids Res* **32**: 3683–3688.
- Salpeter SJ, Klochendler A, Weinberg-Corem N, Porat S, Granot Z, Shapiro AM *et al.* (2011). Glucose regulates cyclin D2 expression in quiescent and replicating pancreatic β -cells through glycolysis and calcium channels. *Endocrinology* **152**: 2589–2598.
- Sartori AA, Lukas C, Coates J, Mistrik M, Fu S, Bartek J *et al.* (2007). Human CtIP promotes DNA end resection. *Nature* **450**: 509–514.
- Schaaf MJ, Cidowski JA. (2003). Molecular determinants of glucocorticoid receptor mobility in living cells: the importance of ligand affinity. *Mol Cell Biol* **23**: 1922–1934.
- Schwartz M, Zlotorynski E, Goldberg M, Ozeri E, Rahat A, le Sage C *et al.* (2005). Homologous recombination and nonhomologous end-joining repair pathways regulate fragile site stability. *Genes Dev* **19**: 2715–2726.
- Shibata A, Conrad S, Birraux J, Geuting V, Barton O, Ismail A *et al.* (2011). Factors determining DNA double-strand break repair pathway choice in G2 phase. *EMBO J* **30**: 1079–1092.
- Shrivastav M, De Haro LP, Nickoloff JA. (2008). Regulation of DNA double-strand break repair pathway choice. *Cell Res* **18**: 134–147.
- Soutoglou E, Dorn JF, Sengupta K, Jasin M, Nussenzweig A, Ried T *et al.* (2007). Positional stability of single double-strand breaks in mammalian cells. *Nat Cell Biol* **9**: 675–682.
- Takashima Y, Sakuraba M, Koizumi T, Sakamoto H, Hayashi M, Honma M. (2009). Dependence of DNA double strand break repair pathways on cell cycle phase in human lymphoblastoid cells. *Environ Mol Mutagen* **50**: 815–822.
- Takata M, Sasaki MS, Sonoda E, Morrison C, Hashimoto M, Utsumi H *et al.* (1998). Homologous recombination and non-homologous end-joining pathways of DNA double-strand break repair have overlapping roles in the maintenance of chromosomal integrity in vertebrate cells. *EMBO J* **17**: 5497–5508.
- Villalobos MJ, Betti CJ, Vaughan AT. (2006). Detection of DNA double-strand breaks and chromosome translocations using ligation-mediated PCR and inverse PCR. *Methods Mol Biol* **314**: 109–121.
- Wersto RP, Chrest FJ, Leary JF, Morris C, Stetler-Stevenson MA, Gabrielson E. (2001). Doublet discrimination in DNA cell-cycle analysis. *Cytometry* **46**: 296–306.
- Yanez RJ, Porter AC. (1998). Therapeutic gene targeting. *Gene Ther* **5**: 149–159.
- Zur A, Brandeis M. (2001). Securin degradation is mediated by fzy and fzr, and is required for complete chromatid separation but not for cytokinesis. *EMBO J* **20**: 792–801.

Supplementary Information accompanies the paper on the Oncogene website (<http://www.nature.com/onc>)